THE BELL SYSTEM TECHNICAL JOURNAL
Vol. 54, No. 3, March 1975
Printed in U.S.A.

Design and Evaluation of Shifted-Companion-Form Active Filters

By J. TOW

(Manuscript received August 12, 1974)

Two techniques for designing a class of low-sensitivity, follow-the-leader, feedback-type active filters have been introduced by Hurtig and Laker-Ghausi. The FLF configuration consists of a cascade of second- and/or first-order sections, with feedback from each section back to the first. This paper presents an approach for designing FLF-type realization for all classes of filter functions. The technique is based on a shifted-companion form of the associated-state equations. Some salient features of Hurtig's primary resonator block, Laker-Ghausi's follow-the-leader feedback, and the shifted-companion-form techniques are presented below.

(*i*) *Hurtig's PRB realizes any all-pole (no finite transmission zeros) filter function. This includes the low-pass, high-pass, and symmetrical bandpass filters without finite zeros. Explicit design equations are available, and the individual sections in the array are identical.*

(*ii*) *Laker-Ghausi's FLF realizes any symmetrical (including finite transmission zeros) bandpass filter function. The sections are not constrained to be identical, which allows optimization using this degree of freedom. Finite zeros are realized by a summation technique.*

(*iii*) *The SCF realizes all types of filter functions, i.e., low-pass, high-pass, bandpass, all-pass, or band-reject filters. Explicit design equations are available. The first section can differ from the rest, thus allowing some optimization with standardization. Feedforward as well as summation techniques can be used to realize the finite zeros.*

Two bandpass design examples using SCF, PRB, and/or Laker-Ghausi FLF techniques are given and compared with the low-sensitivity coupled (leapfrog) biquad, the conventional cascade biquad, and the passive ladder filter designs. The comparison shows that the passive filter gives

the best performance with respect to sensitivity to element deviations. All the coupled designs are significantly better than the cascade design in the passband, with the coupled biquad (leapfrog) design the most significantly better. In the stopband, cascade and coupled designs perform roughly the same.

I. INTRODUCTION

Recently, Hurtig[1,2] introduced a low-sensitivity, multiple-loop-feedback active RC filter configuration for the realization of greater-than-second-order voltage transfer functions. The configuration has been found to exhibit greatly improved stability over cascaded designs. For symmetrical bandpass filters, Hurtig's structure [called the primary resonator block (PRB) configuration] consists of a cascade of identical biquadratic bandpass sections (i.e., same pole-frequency and pole-Q) with feedback from each section (except the first) back to the first section. More recently, Laker and Ghausi[3,4] extended Hurtig's configuration to include symmetrical bandpass filters with finite transmission zeros, e.g., elliptic-type filters. In Laker and Ghausi's approach [called the follow-the-leader feedback (FLF) technique], different pole-Q values can be allowed for the biquadratic bandpass sections.

For the PRB technique, Hurtig has given a set of explicit equations expressing the biquadratic bandpass transfer function and the feedback factors in terms of the coefficients of the all-pole prototype low-pass transfer function.[2] In the FLF approach, Laker and Ghausi used a coefficient-matching technique. Because of the nonuniqueness of solutions in the FLF approach, Laker and Ghausi further proposed a method of choosing the pole-Q values for an optimum design.

In this paper, we present yet another approach based on a shifted-companion form of state variable representation of the voltage transfer function for the design of symmetrical bandpass and band-reject filters with this structure. In the bandpass case, using the proposed method, each biquadratic bandpass section in the cascaded array must be identical, with the possible exception of the first. Hence, it includes the Hurtig PRB configuration as a special case, but does not encompass the Laker-Ghausi cases having three or more different values of pole-Q. As in Laker-Ghausi's approach, the design of symmetrical bandpass filters with finite transmission zeros is included in the discussion of the shifted-companion form. Similarly to Hurtig's approach, the shifted-companion form also gives explicit design formulas as opposed to the coefficient-matching technique used by Laker and Ghausi. Furthermore, in the shifted-companion-form

design, different realizations (with the same configuration) can be obtained by varying the value of a shift parameter. The standard companion-form representation[5] corresponds to the case in which the value of this shift parameter is equal to zero.

In the next section, the shifted-companion-form representation of a voltage transfer function is presented. A brief discussion on the optimal choice of the shift parameter based on our design experience is given in Section III. Two design examples, a three-section Butterworth bandpass filter and a three-section elliptic bandpass filter, are given in Section IV. The section also compares the sensitivity performance, in a Monte-Carlo sense, of the shifted-companion-form designs to the cascade biquad and the coupled biquad[6,7] as well as to the passive designs.

II. SHIFTED-COMPANION-FORM REPRESENTATION OF VOLTAGE TRANSFER FUNCTION

The design technique for the proposed shifted-companion-form representation of a voltage transfer function is obtained as follows. First, a shift is introduced to the complex frequency variable by adding a variable constant α (shift parameter) to the complex frequency variable. Second, the resulting shifted-transfer function is represented by the standard companion form[5] and its corresponding block diagram, which has the desired structure. Third, an inverse shift operation is made on the standard companion form to determine the proper values for the parameters of the structure.

2.1 Representation of voltage transfer function by a shifted-companion form

Let the voltage transfer function be given by

$$\frac{V_{out}}{V_{in}}(p) = \frac{n_m p^m + n_{m-1}p^{m-1} + \cdots + n_1 p + n_0}{p^n + d_{n-1}p^{n-1} + \cdots + d_1 p + d_0} + d, \quad \text{for } m < n. \tag{1}$$

Let the following shifting be made in the complex frequency variable of (1):

$$p = s - \alpha, \tag{2}$$

where α, the shift parameter, is a real number. Substitution of (2) into (1) results in the following shifted-transfer function (see Appendix A):

$$\frac{V_{out}}{V_{in}}(s) = \frac{\sum_{i=0}^{m} b_{m-i}s^{m-i}}{s^n + \sum_{j=1}^{n} a_{n-j}s^{n-j}} + d, \tag{3}$$

where

$$\left.\begin{aligned} a_{n-j} &= \sum_{k=0}^{j} (-1)^{j-k} \frac{(n-k)!}{(j-k)!(n-j)!} \alpha^{j-k} d_{n-k}, \\ & \qquad\qquad j = 1, 2, \cdots, n \\ b_{m-i} &= \sum_{k=0}^{i} (-1)^{i-k} \frac{(m-k)!}{(i-k)!(m-i)!} \alpha^{i-k} n_{m-k}, \\ & \qquad\qquad i = 0, 1, \cdots, m \end{aligned}\right\}. \tag{3a}$$

Note that $d_n = 1$. Alternatively, the a's and b's can also be obtained by the following implicitly recursive formula:

$$\left.\begin{aligned} a_n &= 1 \\ d_{n-j} &= \sum_{k=0}^{j} \frac{(n-k)!}{(j-k)!(n-j)!} \alpha^{j-k} a_{n-k}, \qquad j = 1, 2, \cdots, n \\ n_{m-i} &= \sum_{k=0}^{i} \frac{(m-k)!}{(i-k)!(m-i)!} \alpha^{i-k} b_{m-k}, \qquad i = 0, 1, \cdots, m \end{aligned}\right\}. \tag{3b}$$

It is well known that a voltage transfer function (with degree n) can be represented by a set of state equations in the (standard) companion form,[5] i.e.,

$$\begin{aligned} \dot{\mathbf{x}} &= \mathbf{A}\mathbf{x} + \mathbf{b}v_{\text{in}} \\ v_{\text{out}} &= \mathbf{c}\mathbf{x} + dv_{\text{in}}, \end{aligned} \tag{4}$$

where the state matrix $\mathbf{A}$ is of dimension $n \times n$. In the case of eq. (3), we have

$$\left.\begin{aligned} \mathbf{x} &= (x_1, x_2, \cdots, x_n)^t \\ \mathbf{A} &= \begin{bmatrix} -a_{n-1} & -a_{n-2} & -a_{n-3} & \cdots & -a_1 & -a_0 \\ 1 & 0 & 0 & \cdots & 0 & 0 \\ 0 & 1 & 0 & \cdots & 0 & 0 \\ & & & \vdots & & \\ 0 & 0 & 0 & \cdots & 1 & 0 \end{bmatrix}, \qquad \mathbf{b} = \begin{bmatrix} \beta_1 \\ \beta_2 \\ \vdots \\ \beta_n \end{bmatrix} \\ \mathbf{c} &= [\gamma_1, \gamma_2, \cdots, \gamma_n]. \end{aligned}\right\} \tag{5}$$

There are two special cases for eq. (5), A and B.

Case A: Transmission-zero forming by an input feed-forward technique:

$$\begin{aligned} \mathbf{c} &= [0\ 0\ \cdots\ 1] \\ \mathbf{b} &= [\beta_1\ \beta_2\ \cdots\ \beta_n]^t \end{aligned}$$

and

$$\beta_{n+1-i} = b_{n-i} - \sum_{j=1}^{i-1} a_{n-i+j}\beta_{n+1-j}, \qquad i = 1, 2, \cdots, n. \tag{5a}$$

Case B: Transmission-zero forming by summation-of-state-variables technique:

$$\begin{aligned} \mathbf{b} &= [1\ 0\ \cdots\ 0]^t \\ \mathbf{c} &= [b_{n-1}\ b_{n-2}\ \cdots\ b_0]. \end{aligned} \tag{5b}$$

To obtain the shifted-companion-form representation of the voltage transfer function of eq. (1), the inverse shift operation, i.e., $s = p + \alpha$ is applied to eq. (4). This is equivalent to the following operation:

$$\begin{array}{c|c|c} \text{time domain} & \text{frequency domain} & \text{time domain} \\ \dot{\mathbf{x}} \Leftrightarrow s\mathbf{X} \xrightarrow[s=p+\alpha]{\text{inverse shift}} (p+\alpha)\mathbf{X} & & \Leftrightarrow \dot{\mathbf{x}} + \alpha\mathbf{I}\mathbf{x}, \end{array} \tag{6}$$

where $\mathbf{I}$ is the $n \times n$ identity matrix. Hence, a shifted-companion-form representation of eq. (1) is*

$$\begin{aligned} \dot{\mathbf{y}} &= \mathbf{A}'\mathbf{y} + \mathbf{b}v_{\text{in}} \\ v_{\text{out}} &= \mathbf{c}\mathbf{y} + dv_{\text{in}}, \end{aligned} \tag{7}$$

where

$$\mathbf{A}' = \mathbf{A} - \alpha\mathbf{I} = \begin{bmatrix} -a_{n-1} - \alpha & -a_{n-2} & -a_{n-3} & \cdots & -a_1 & -a_0 \\ 1 & -\alpha & 0 & \cdots & 0 & 0 \\ 0 & 1 & -\alpha & \cdots & 0 & 0 \\ & & & \vdots & & \\ 0 & 0 & 0 & \cdots & 1 & -\alpha \end{bmatrix}, \tag{7a}$$

and the vectors $\mathbf{b}$ and $\mathbf{c}$ are as given in eqs. (5a) or (5b).

At this point, it is desirable to change the relative level of the state vector $\mathbf{y}$ to obtain more convenient values for the gain (i.e., close to unity) of the individual biquadratic sections. Mathematically, we let

$$\mathbf{y} = \mathbf{K}\mathbf{x}, \tag{8}$$

where $\mathbf{K}$ is a nonsingular diagonal matrix. It has been found convenient to choose $\mathbf{K}$ to have the following form:

$$\mathbf{K} = \text{diag}\,[\alpha^{n-1}\ \ \alpha^{n-2}\ \ \cdots\ \ \alpha\ \ 1]. \tag{9}$$

Substituting (8) and (9) into (7) and (7a), the following shifted-companion-form representation of eq. (1) is obtained:

$$\begin{aligned} \dot{\mathbf{x}} &= \hat{\mathbf{A}}\mathbf{x} + \hat{\mathbf{b}}v_{\text{in}} \\ v_{\text{out}} &= \hat{\mathbf{c}}\mathbf{x} + dv_{\text{in}}, \end{aligned} \tag{10}$$

---

* The state vector is changed from $\mathbf{x}$ to $\mathbf{y}$.

where

$$\hat{\mathbf{A}} = \mathbf{K}^{-1}\mathbf{A}'\mathbf{K} = \begin{bmatrix} -a_{n-1} - \alpha & -\frac{a_{n-2}}{\alpha} & -\frac{a_{n-3}}{\alpha^2} & \cdots & -\frac{a_1}{\alpha^{n-2}} & -\frac{a_0}{\alpha^{n-1}} \\ \alpha & -\alpha & 0 & \cdots & 0 & 0 \\ 0 & \alpha & -\alpha & \cdots & 0 & 0 \\ & & & \vdots & & \\ 0 & 0 & 0 & \cdots & \alpha & -\alpha \end{bmatrix} \tag{11}$$

$$\hat{\mathbf{b}} = \mathbf{K}^{-1}\mathbf{b} = \left[\frac{\beta_1}{\alpha^{n-1}} \quad \frac{\beta_2}{\alpha^{n-2}} \quad \cdots \quad \frac{\beta_{n-1}}{\alpha} \quad \beta_n\right]^t$$

$$\hat{\mathbf{c}} = \mathbf{c}\mathbf{K} = [0 \quad 0 \quad \cdots \quad 0 \quad 1] \tag{11a}$$

or

$$\hat{\mathbf{b}} = \mathbf{K}^{-1}\mathbf{b} = \left[\frac{1}{\alpha^{n-1}} \quad 0 \quad \cdots \quad 0 \quad 0\right]^t$$

$$\hat{\mathbf{c}} = \mathbf{c}\mathbf{K} = [\alpha^{n-1}b_{n-1} \quad \alpha^{n-2}b_{n-2} \quad \cdots \quad \alpha b_1 \quad b_0]. \tag{11b}$$

Equations (11a) and (11b) correspond to the cases where the transmission zeros are formed by the input feed-forward and the summation techniques, respectively.

2.2 Block diagram representation of the shifted-companion form

Transforming eqs. (10), (11), and (11a) into the frequency domain, the following set of transfer functions representing the shifted-companion form is obtained.

$$\left.\begin{aligned} X_1(p) &= \frac{1}{p + (a_{n-1} + \alpha)}\left[-\sum_{j=2}^{n}\frac{a_{n-j}}{\alpha^{j-1}}X_j(p) + \frac{\beta_1}{\alpha^{n-1}}V_{\text{in}}(p)\right] \\ X_i(p) &= \frac{1}{p + \alpha}\left[\alpha X_{i-1}(p) + \frac{\beta_i}{\alpha^{n-i}}V_{\text{in}}(p)\right] \qquad \text{for} \quad i = 2, 3, \cdots, n \\ V_{\text{out}}(p) &= X_n(p) + dV_{\text{in}}(p) \end{aligned}\right\}. \tag{12}$$

Similarly, by transforming eqs. (10), (11), and (11b), we have

$$\left.\begin{aligned} X_1(p) &= \frac{1}{p + (a_{n-1} + \alpha)}\left[-\sum_{j=2}^{n}\frac{a_{n-j}}{\alpha^{j-1}}X_j(p) + \frac{1}{\alpha^{n-1}}V_{\text{in}}(p)\right] \\ X_i(p) &= \frac{1}{p + \alpha}[\alpha X_{i-1}(p)] \quad \text{for} \quad i = 2, 3, \cdots, n \\ V_{\text{out}}(p) &= \sum_{i=1}^{n}\alpha^{n-i}b_{n-i}X_i(p) + dV_{\text{in}}(p) \end{aligned}\right\}. \tag{13}$$

Equations (12) and (13) are shown in block diagram form in Figs. 1a and 1b, respectively.

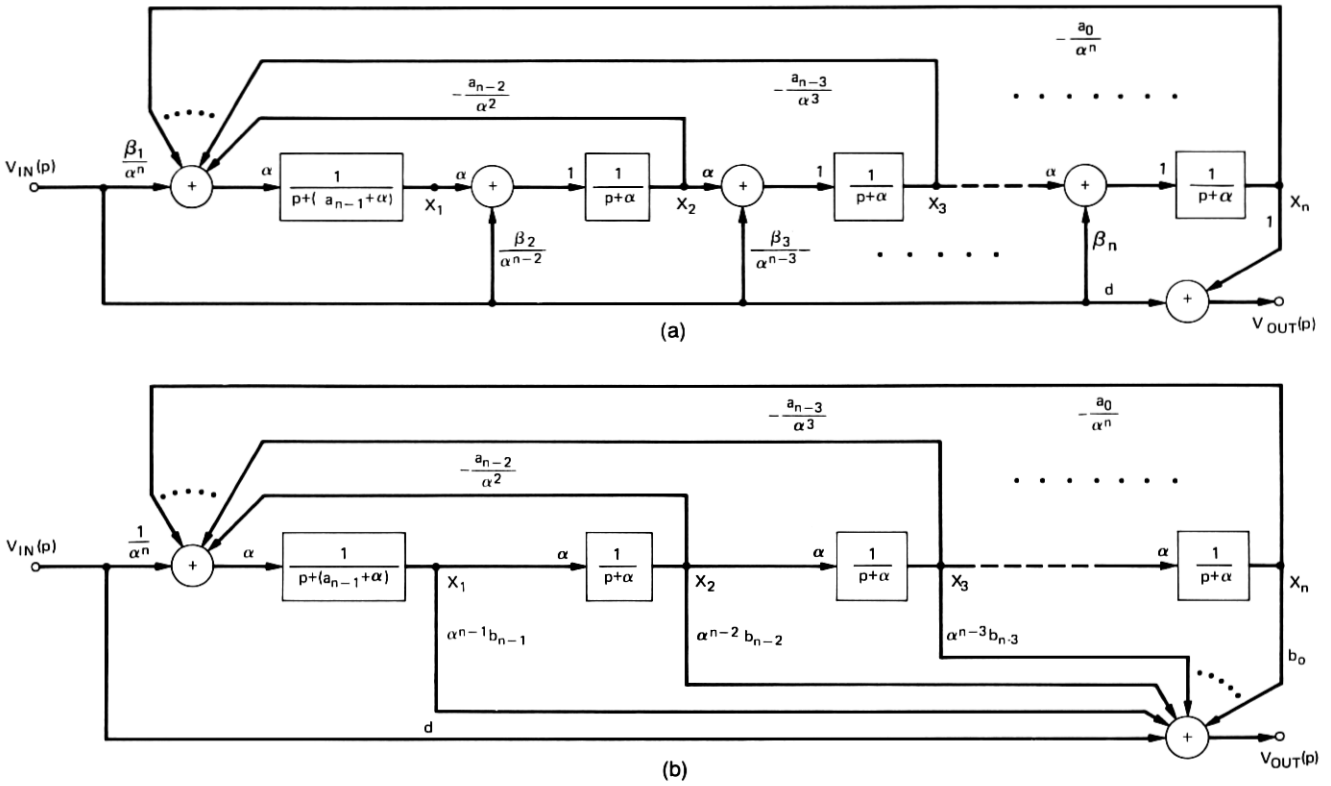

Fig. 1—Shifted-companion form. (a) Feed-forward zero-forming technique. (b) Summation zero-forming technique.

2.3 Block diagram representation of symmetrical bandpass filters via the shifted-companion form

For geometrically symmetrical bandpass filters, eq. (1), eq. (12) or (13), and Fig. 1a or 1b can be taken as the transfer function, the shifted-companion-form representation, and the block-diagram representation of the corresponding low-pass prototype, respectively. To obtain the block diagram representation of the symmetrical bandpass filter transfer function, we can apply the well-known low-pass to bandpass transformation:

$$p = \frac{s^2 + \omega_0^2}{Bs}, \tag{14}$$

where

p = complex frequency for the normalized low-pass function
s = complex frequency for the actual bandpass function
ω_0 = center frequency of the bandpass filter (in radians/s)
B = passband bandwidth of the bandpass filter (in radians/s)

to Figs. 1a and 1b. The resulting block diagram representations are shown in Figs. 2a and 2b.

2.4 Block diagram representation of symmetrical band-reject filters via the shifted-companion form

To obtain the block diagram representation of the symmetrical band-reject filter transfer function, similarly to the development of Section 2.3, we can first apply a low-pass to high-pass transformation, then follow with the usual low-pass to bandpass transformation, eq. (14). Specifically, this results in the following transformation to Figs. 1a and 1b:

$$\frac{1}{p + \alpha} = \frac{1}{\alpha} \cdot \frac{s^2 + \omega_0^2}{s^2 + (B/\alpha)s + \omega_0^2}, \tag{15}$$

where

p = complex frequency for the normalized low-pass function
s = complex frequency for the actual band-reject function
ω_0 = $\sqrt{\omega_2 \omega_1}$ (in radians/s)
B = $\omega_2 - \omega_1$ (in radians/s)
ω_1/ω_2 = the lower/upper passband edge frequencies of the band-reject filter.

The resulting block diagram representation can also be shown as in Fig. 2, except that

$$T_1(s) = \frac{1}{a_{n-1} + \alpha} \cdot \frac{s^2 + \omega_0^2}{s^2 + [Bs/(a_{n-1} + \alpha)] + \omega_0^2}$$

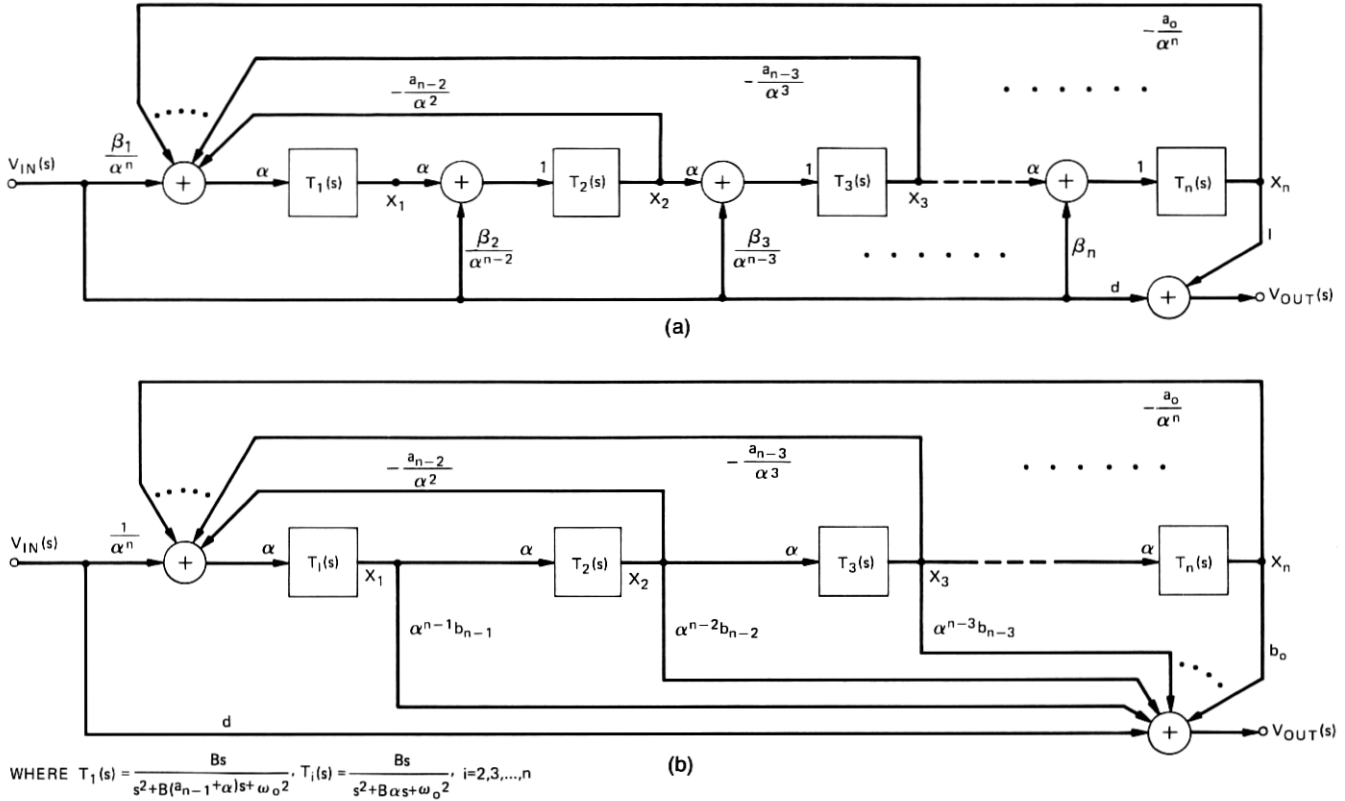

Fig. 2—Symmetrical bandpass filters via the shifted-companion form. (a) Feed-forward zero-forming technique. (b) Summation zero-forming technique.

and

$$T_i(s) = \frac{1}{\alpha} \cdot \frac{s^2 + \omega_0^2}{s^2 + (B/\alpha)s + \omega_0^2}, \qquad i = 2, 3, \cdots, n.$$

In passing, we note that Fig. 2 can also represent the symmetrical band-reject filter provided the parameters in Fig. 2 are determined by making eq. (1) the transfer function of the band-reject's corresponding high-pass prototype.

III. OPTIMAL CHOICE OF THE SHIFT PARAMETER, α

For symmetrical bandpass filters (Fig. 2), it is seen that all the biquadratic sections, with the possible exception of the first section, have a pole-Q value equal to $\omega_0/B\alpha$. The pole-Q value for the first section is

$$\frac{\omega_0}{B(a_{n-1} + \alpha)} \quad \text{or} \quad \frac{\omega_0}{B[d_{n-1} - (n-1)\alpha]}.$$

The value of these Q's versus α is illustrated in Fig. 3.

Before we proceed with a discussion on the optimal choice of α, two special cases are pointed out. The first is the standard companion form which corresponds to the case where $\alpha = 0$. From Eq. (3a),

$$a_{n-1} = d_{n-1} - n\alpha. \tag{16}$$

Letting $\alpha = d_{n-1}/n$, $a_{n-1} = 0$. With this value, (d_{n-1}/n) for α, a second special case is obtained where all the biquadratic sections (including the first) will have a pole-Q value equal to $\omega_0/B \cdot n/(d_{n-1})$. For simple symmetrical bandpass filters, this special case reduces to Hurtig's PRB configuration, and Hurtig's design formula[2] is identical to that given by eq. (3b).

Since an infinite number of realizations, depending upon the choice of α, can be obtained for the shifted-companion-form representation, is there an optimal choice of α? This optimal choice would, perhaps, depend also upon the performance criterion chosen. Laker and Ghausi have proposed an optimization scheme for their configuration based on a minimization of a certain statistical multiparameter sensitivity measure.[3,4] Their scheme can also be used here for the determination of an optimal α with respect to their performance criterion. In the following, we present two observations based on our limited design experience with bandpass filters using the proposed shifted-companion form where minimizing the filter's passband sensitivity is of primary concern. In our discussion here, the filter designs are subjected to a computer-simulated Monte-Carlo analysis and sensitivity is examined from the standpoint of standard deviation (dB) vs frequency.

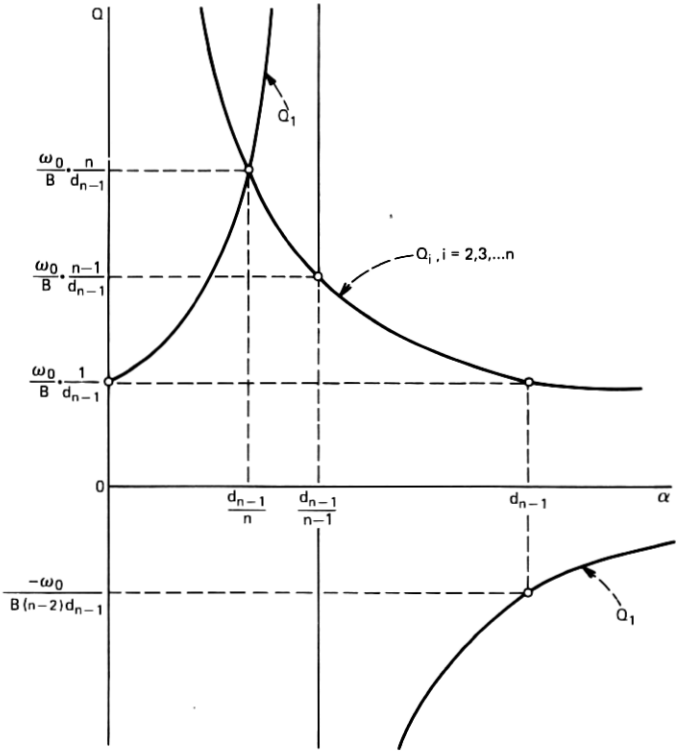

Fig. 3—Biquadratic sections Q vs shift parameter α.

(*i*) It appears that a broad range of values exists for α where the improvements* over the cascade biquad design are relatively constant. This range includes Hurtig's design, i.e., $\alpha = d_{n-1}/n$.

(*ii*) Performance of the standard companion-form (i.e., $\alpha = 0$) design is about the same as that of the cascade biquad design.

The above empirical rule (*i*) is observed in the design examples to follow.

IV. DESIGN EXAMPLES

Two examples given here illustrate the shifted-companion-form design technique as well as demonstrate its performance relative to that of the cascade biquad, coupled (leapfrog) biquad as well as to passive ladder designs. Comparisons among these designs are based on a Monte-Carlo analysis of the filters with passive components selected randomly from a uniform distribution within a given tolerance interval.

* Improvement is to be broadly interpreted as less sensitive or having a smaller standard deviation.

4.1 Example 1—A three-section Butterworth bandpass filter*

The normalized transfer function of a third-order low-pass Butterworth filter is given by

$$\frac{V_{out}}{V_{in}}(p) = \frac{1}{p^3 + 2p^2 + 2p + 1}. \tag{17}$$

Let the desired bandpass filter have center frequency (f_0) of 1 Hz and 3-dB bandwidth ($B/2\pi$) of 0.04 Hz. The PRB version of the shifted-companion form is designed here. Hence,

$$\alpha = \frac{d_{n-1}}{n} = \frac{2}{3}.$$

From eq. (3a), we obtain

$$a_2 = 0, \quad a_1 = 0.66666667, \quad a_0 = 0.25925926$$
$$b_2 = b_1 = 0, \quad b_0 = 1.$$

And from eq. (5a),

$$\beta_1 = 1, \quad \beta_2 = 0, \quad \beta_3 = 0.$$

For this simple bandpass filter, the output summing amplifier (Fig. 2) is not needed. Furthermore,

$$\alpha T_i(s) = \frac{0.08\pi(\frac{2}{3})s}{s^2 + 0.08\pi(\frac{2}{3})s + (2\pi)^2} \qquad i = 1, 2, 3.$$

Note that

$$Q_i = \frac{2\pi}{0.08\pi} \cdot \frac{3}{2} = 37.5 \qquad \text{for} \qquad i = 1, 2, 3.$$

For this example, each of the $T_i(s)$ is chosen to be realized by the single-amplifier biquad (SAB) configuration of Ref. 8. The complete configuration† is shown in Fig. 4, with the element values tabulated in Appendix B. The element values as well as circuit topologies for the cascade SAB, coupled SAB (or leapfrog SAB),‡ and the optimized Laker-Ghausi design[3] are also given in Appendix B. Each of the three biquadratic bandpass sections in the shifted-companion-form, Laker-Ghausi, and coupled-biquad designs has a pole frequency of 1 Hz; whereas for the cascade design, the pole frequencies are 1, 1.01747, and 0.982828 Hz. The pole-Q values for these four designs are tabu-

---

* This example can also be found in Ref. 3.

† The inverting amplifier A_2 can be eliminated by feeding the output of section 3 to the positive input terminal of the summing amplifier A_1. This has not been done in the example.

‡ For symmetrical bandpass filters derived from an all-pole low-pass prototype, the coupled biquad and the leapfrog designs can be made identical.

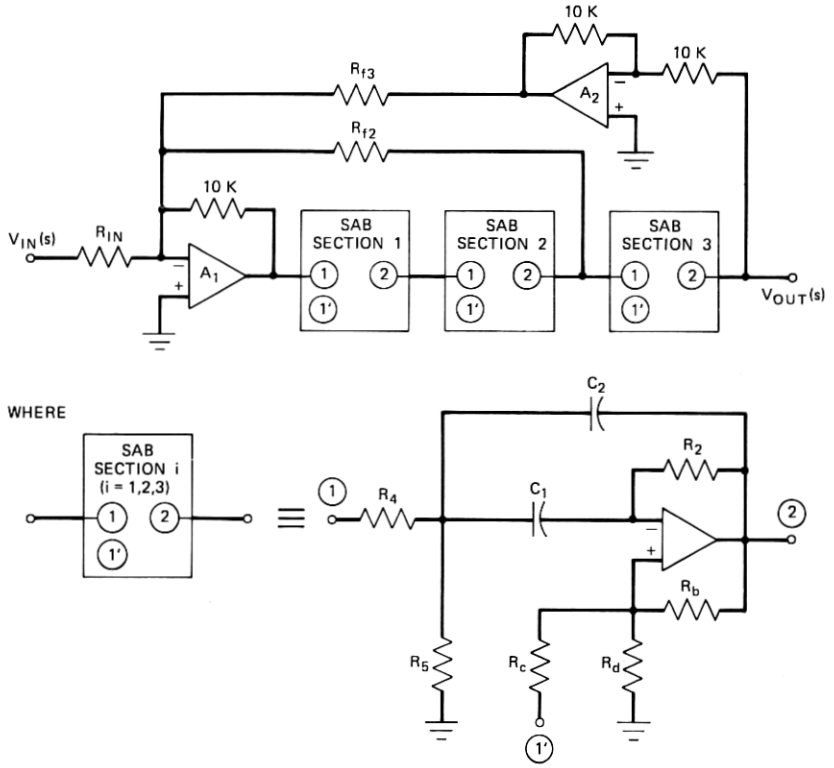

Fig. 4—Configuration for the three-section Butterworth bandpass filter.

lated in Table I. These four realizations of the Butterworth filter as well as the passive ladder realization were compared by a Monte-Carlo study (with 200 trials) using the computer program BELTAP.[9] The following assumptions are made:

(*i*) The operational amplifiers are ideal.
(*ii*) All passive components have the same tolerance with a uniform distribution.

Table I — Pole-Q values for the three-section Butterworth filter

Filter Type \ Pole-Q	Section		
	1	2	3
Shifted-companion form (PRB)	37.5	37.5	37.5
Laker-Ghausi (FLF)	44.2	44.2	28.8
Cascade biquad	25.0	50.0075	50.0075
Coupled biquad/leapfrog	25.0	∞	25.0

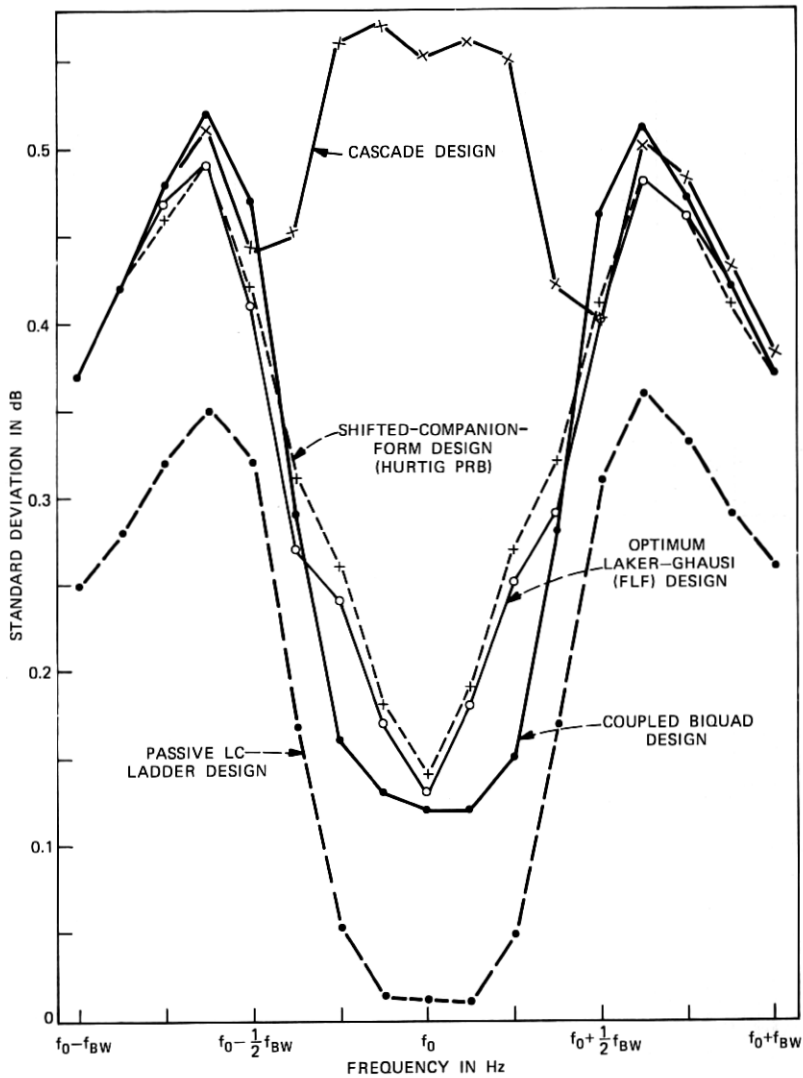

Fig. 5—Simulated variations of the three-section Butterworth bandpass filter (0.1732-percent passive components tolerance).

Two different tolerances were simulated, the first having a realistic tolerance of ± 0.1732 percent and the second a large tolerance of ± 1.732 percent.* The resulting comparisons based on the standard

* Realistic in the sense that the statistical variation of the filter response is within a reasonable bound from the nominal. The large tolerance corresponds to a component standard deviation of 1 percent, which was used in the example of Ref. 3.

deviations of the transfer function (dB) of the various designs plotted vs frequency (Hz) are shown in Figs. 5 and 6.

It is observed that, over most of the passband (between the 3-dB points), the coupled biquad/leapfrog, Hurtig's PRB/shifted-companion form, and Laker-Ghausi FLF designs show roughly the same improvement (3-to-1 reduction in standard deviations) over the cascade biquad design. The passive filter is, however, seen to be the least sensitive.

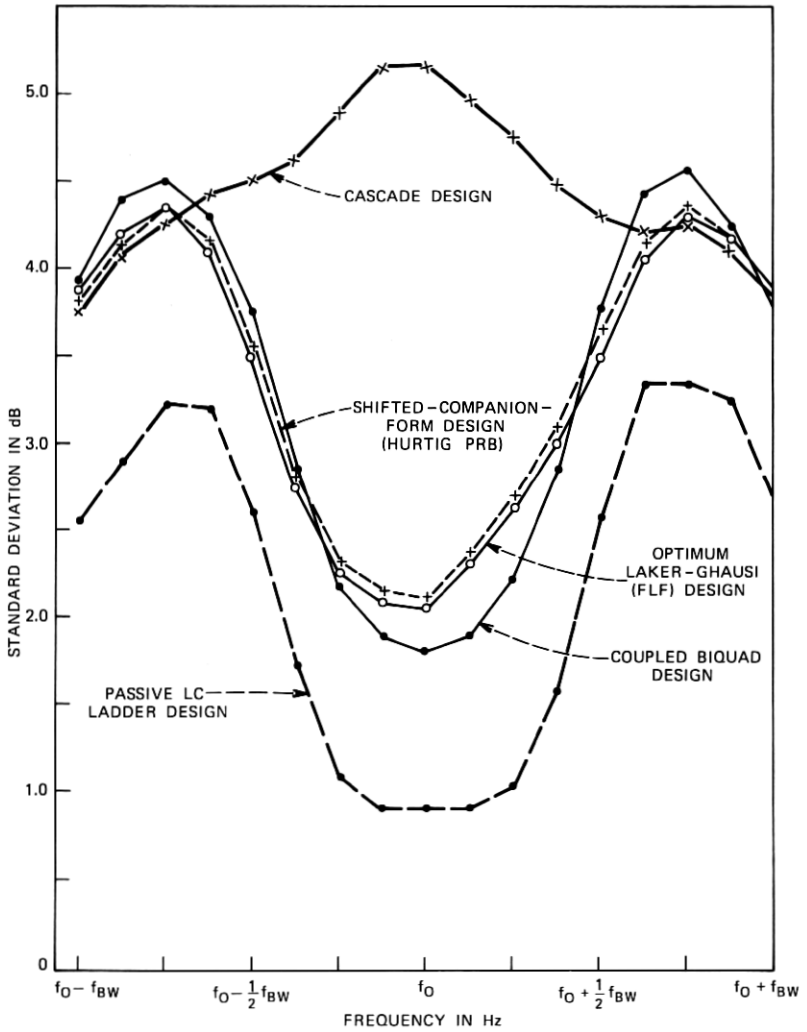

Fig. 6—Simulated variations of the three-section Butterworth bandpass filter (1.732-percent passive components tolerance).

4.2 Example 2—A three-section elliptic bandpass filter*

A sixth-order elliptic bandpass filter with center frequency (f_0) at 2805 Hz, 0.1-dB passband ripple with bandwidth ($B/2\pi$) of 90 Hz, and a minimum 30-dB loss below 2694.8 Hz and above 2919.8 Hz is desired. The corresponding third-order normalized low-pass prototype transfer function is given by

$$\frac{V_{\text{out}}}{V_{\text{in}}}(p) = \frac{N(p)}{D(p)},$$

where

$$N(p) = 0.214115(p^2 + 8.158500)$$
$$D(p) = p^3 + 1.897376p^2 + 2.543168p + 1.746858.$$

Once again, the Hurtig criterion is used for the shifted-companion-form design. Hence,

$$\alpha = \frac{d_2}{3} = 0.6324587.$$

From eq. (3a),

$$a_2 = 0, \quad a_1 = 1.3431556, \quad a_0 = 0.64438116$$
$$b_2 = 0.214115, \quad b_1 = -0.2708378, \quad b_0 = 1.8325041.$$

And from eq. (5a),

$$\beta_1 = 1.5449143, \quad \beta_2 = -0.2708378, \quad \beta_3 = 0.214115.$$

The feed-forward zero-forming configuration (Fig. 2a) is used for the realization† where

$$T_i(s) = \frac{180\pi s}{s^2 + 180\pi(0.6324587)s + (2\pi \cdot 2805)^2}.$$

For this example, each of the $T_i(s)$ is chosen to be realized by the three-amplifier biquad configuration.[10] The complete configuration‡ is shown in Fig. 7 with the element values tabulated in Appendix C. The element values for the cascade biquad and coupled biquad designs are also given in Appendix C.§ A leapfrog design is also available,[11] the performance of which is similar to but slightly inferior to the coupled biquad design. Once again, a Monte-Carlo study was made on these

---

* This example can also be found in Ref. 6.

† It was found, for this example, that the design with the feed-forward zero-forming technique outperforms the summation zero-forming technique design.

‡ With the three-amplifier biquad sections, it is possible to eliminate the input summing amplifier A_1 by using node 1 of section 1 as the summing point. This has not been done in the example.

§ Without the availability of a computer program to choose an optimized Laker-Ghausi circuit, no FLF design is included in this example.

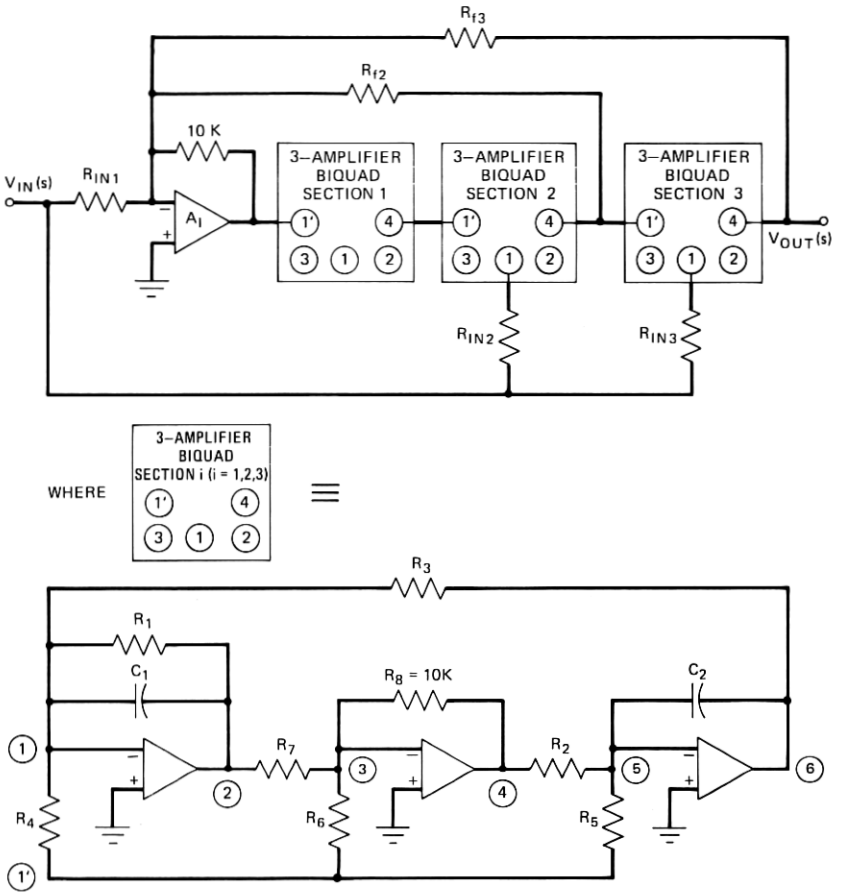

Fig. 7—Configuration for the three-section elliptic bandpass filter.

designs as well as a passive ladder design. The resulting comparisons are shown in Figs. 8 and 9, where a 0.25-percent tolerance (with uniform distribution) is assumed for all passive components.

It is observed that, in terms of standard deviation, the passband improvements over the cascade design are noticeably less for the shifted-companion-form (α chosen by Hurtig's PBR criterion) design than the roughly 4-to-1 improvement of the coupled biquad design. Once again, the passive filter outperforms its active counterparts.

V. CONCLUSIONS

The FLF/PRB multiple-loop feedback active filter structure is known to have better sensitivity performance than the popular cascade approach. This sensitivity improvement is particularly acute in high-Q

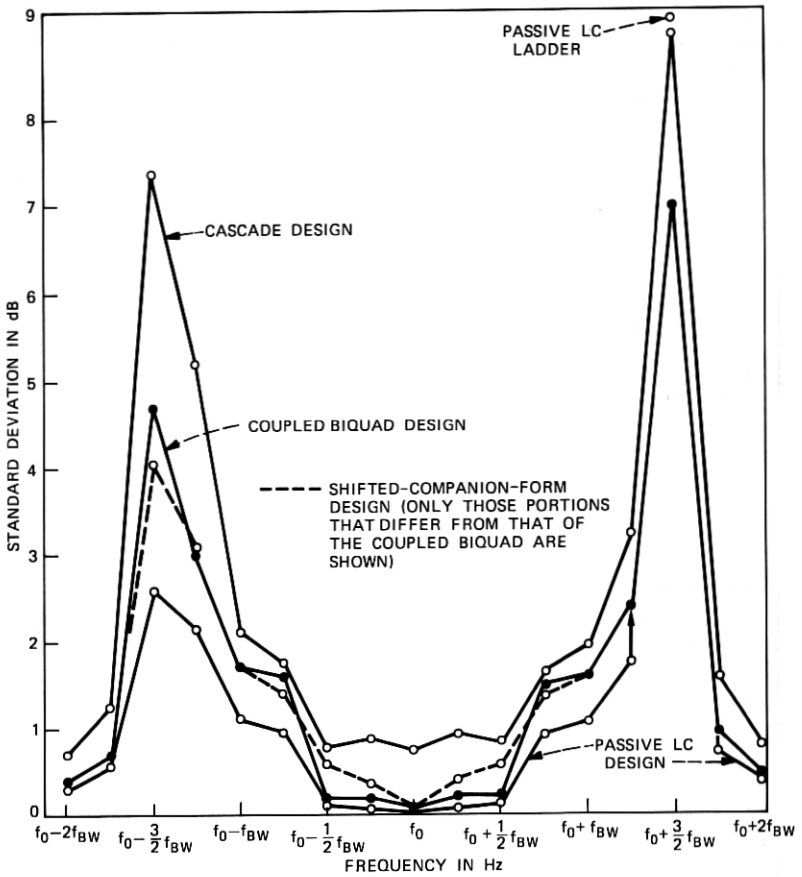

Fig. 8—Simulated variations of the elliptic bandpass filter.

bandpass filter designs, as exemplified in the two examples given. With the described shifted-companion-form representation of the filter transfer function, it is straightforward to obtain explicit design formulas for this feedback structure as contrasted to the coefficient matching technique used by Laker and Ghausi. In practice, the shift parameter can be chosen such that identical biquadratic blocks (i.e., the extended PRB version)* are used. The proposed shifted-companion-form design has the following advantages over the optimized FLF design. First, no matrix inversion and involved sensitivity minimization routine are needed. Second, all sections are identical, and the sections' pole-Q can be much lower than the highest pole-Q required for the FLF design. Furthermore, little difference is usually observed for this shifted-

* Hurtig's PRB does not treat the cases with finite transmission zeros.

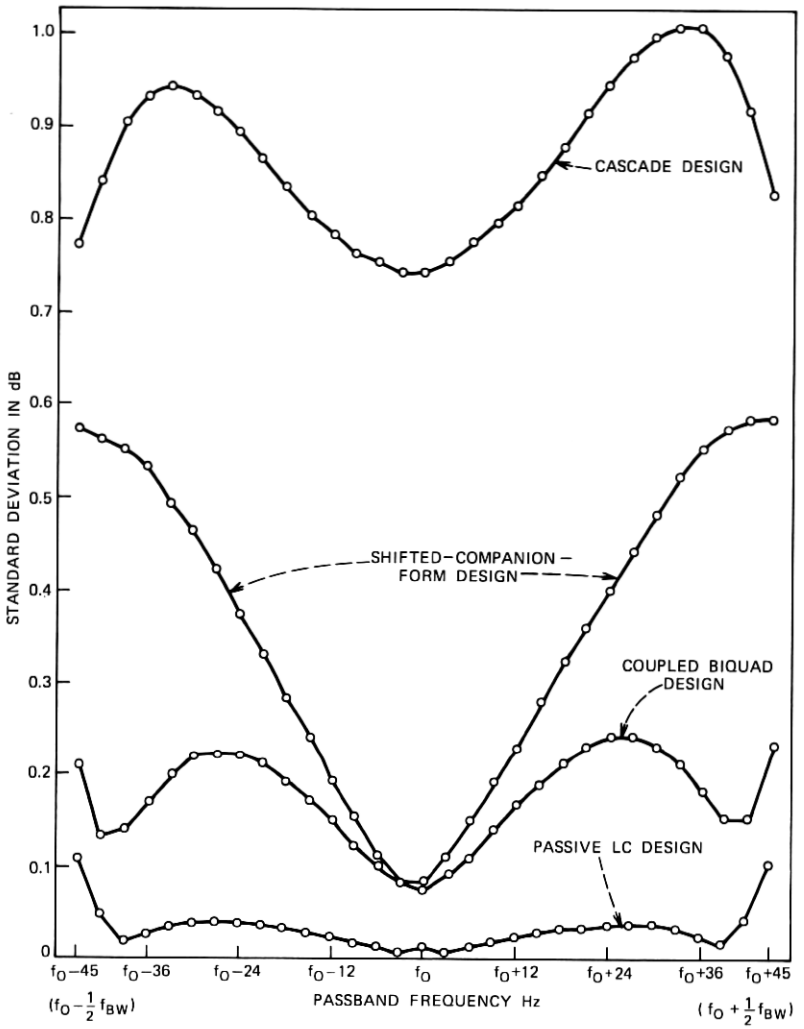

Fig. 9—Simulated variations (passband) of the elliptic bandpass filters.

companion-form design and the optimized FLF design. On the other hand, the two examples also show that the coupled biquad and leapfrog designs may have better sensitivity performance than the corresponding shifted-companion-form designs. However, for those types of filter functions having finite transmission zeros, the designs of coupled biquad and/or leapfrog require extensive computer aids that are not yet generally available. Hence, the proposed shifted-companion-form technique may provide an alternative to the coupled biquad/leapfrog active filter design techniques.

VI. ACKNOWLEDGMENT

The author wishes to thank R. C. Drechsler for helpful discussions.

APPENDIX A

Derivation of the Shifted Transfer Function

Let the polynomial $P(p)$ be

$$P(p) = \sum_{i=0}^{n} d_{n-i}p^{n-i}, \tag{18}$$

and let

$$p = s - \alpha. \tag{19}$$

Then

$$\begin{aligned} P(s) &= \sum_{i=0}^{n} d_{n-i}(s-\alpha)^{n-i} \\ &= \sum_{i=0}^{n} d_{n-i} \sum_{r=0}^{n-i} \binom{n-i}{r} s^{n-i-r}(-\alpha)^r, \end{aligned} \tag{20}$$

where

$$\binom{n-i}{r} = \frac{(n-i)!}{r!(n-i-r)!}. \tag{21}$$

Equation (20) can be rearranged in decreasing power of s as follows:

$$\begin{aligned} P(s) = d_n s^n &+ s^{n-1}\left[\sum_{r=0}^{1}\binom{n-r}{1-r}(-\alpha)^{1-r}d_{n-r}\right] \\ &+ s^{n-2}\left[\sum_{r=0}^{2}\binom{n-r}{2-r}(-\alpha)^{2-r}d_{n-r}\right] \\ &+ \cdots + s^{n-i}\sum_{r=0}^{i}\binom{n-r}{i-r}(-\alpha)^{i-r}d_{n-r} \\ &+ \cdots + \sum_{r=0}^{n}\binom{n-r}{n-r}(-\alpha)^{n-r}d_{n-r}. \end{aligned}$$

Or

$$\begin{aligned} P(s) &= \sum_{i=0}^{n} s^{n-i}\left[\sum_{r=0}^{i}(-1)^{i-r}\binom{n-r}{i-r}\alpha^{i-r}d_{n-r}\right] \\ &= \sum_{i=0}^{n} a_{n-i}s^{n-i}, \end{aligned} \tag{22}$$

where

$$a_{n-i} = \sum_{r=0}^{i}(-1)^{i-r}\binom{n-r}{i-r}\alpha^{i-r}d_{n-r},$$

or

$$= \sum_{r=0}^{i}(-1)^{i-r}\frac{(n-r)!}{(i-r)!(n-i)!}\alpha^{i-r}d_{n-r}. \tag{23}$$

Equation (23) can be used to obtain the coefficients of the shifted polynomial $P(s)$ from the coefficients of the polynomial $P(p)$.

Similarly, if we start with the polynomial

$$P(s) = \sum_{i=0}^{n} a_{n-i} s^{n-i} \tag{24}$$

and let

$$s = p + \alpha, \tag{25}$$

then we obtain

$$P(p) = \sum_{i=0}^{n} d_{n-i} p^{n-i},$$

where

$$d_{n-i} = \sum_{r=0}^{i} \frac{(n-r)!}{(i-r)!(n-i)!} \alpha^{i-r} a_{n-r}. \tag{26}$$

APPENDIX B

Element Values for Example 1 (Fig. 4)

For the various realizations, resistors are in kilohms and all capacitor values are 10 μF.

B.1 Shifted-companion-form (Hurtig's) realization

Element \ Section	1	2	3
R_2	128.5	128.5	128.5
R_4	613.2	613.2	613.2
R_5	1.977	1.977	1.977
R_b	73.07	73.07	73.07
R_d	2.0	2.0	2.0
R_c	∞	∞	∞

and $R_{in} = 2.963$, $R_{f2} = 6.667$, $R_{f3} = 11.43$.

B.2 Laker-Ghausi realization

Element \ Section	1	2	3
R_2	128.5	128.5	127.7
R_4	722.3	722.3	470.9
R_5	1.976	1.976	1.993
R_b	71.77	71.78	74.73
R_d	2.0	2.0	2.0
R_c	∞	∞	∞

and $R_{in} = 2.781$, $R_{f2} = 4.600$, $R_{f3} = 23.73$.

B.3 Cascade realization

The summing amplifier A_1 and inverter A_2 are not needed, and the input goes directly to node 1 of section 1.

Element \ Section	1	2	3
R_2	128.5	126.3	130.8
R_4	408.1	409.1	409.1
R_5	1.981	1.946	2.015
R_b	77.76	70.93	70.93
R_d	2.0	2.0	2.0
R_c	∞	∞	∞

B.4 Coupled biquad realization

The summing amplifier A_1 and inverter A_2 are not needed, and the input goes directly to node 1 of section 1.

Element \ Section	1	2	3
R_2	128.5	128.4	128.5
R_4	204.1	820.2	408.1
R_5	1.990	1.977	1.981
R_b	77.39	64.98	77.76
R_d	2.0	2.0	2.0
R_c	414.1	829.8	∞

In addition, node 1′ of section 1 is connected to node 2 of section 2 and node 1′ of section 2 is connected to node 2 of section 3.

APPENDIX C

Element Values for Example 2 (Fig. 7)

For the various realizations, resistors are in kilohms and all capacitor values are 0.01 μF.

C.1 Shifted-companion-form (Hurtig's criterion) realization

Element \ Section	1	2	3
R_1	279.6	279.6	279.6
R_2	5.674	5.674	5.674
R_3	5.674	5.674	5.674
R_4	279.6	279.6	279.6
R_5	∞	∞	∞
R_6	∞	∞	∞
R_7	10.0	10.0	10.0

and

$$R_{f2} = 2.978, \qquad R_{f3} = 3.926$$
$$R_{in1} = 1.638, \qquad R_{in2} = 413.0, \qquad R_{in3} = -825.9.^*$$

C.2 Cascade realization

The summing amplifier A_1 and all input feed-forward paths (R_{in}'s) are not needed. The input goes directly to node 1′ of section 1.

Element \ Section	1	2	3
R_1	167.5	428.6	412.2
R_2	5.674	5.786	5.564
R_3	5.674	5.786	5.564
R_4	167.5	1190.0	732.2
R_5	∞	16.93	9.378
R_6	∞	27.75	17.76
R_7	10.0	10.0	10.0

C.3 Coupled biquad realization

The summing amplifier A_1 is not needed. The input, V_{in}, goes directly into node 1′ of section 1 and nodes 1 of sections 2 and 3 through the feed-forward resistors R_{in2} and R_{in3}, respectively.

Element \ Section	1	2	3
R_1	311.5	∞	133.0
R_2	5.674	5.674	5.674
R_3	5.674	5.674	5.674
R_4	97.92	∞	∞
R_5	∞	∞	∞
R_6	∞	∞	∞
R_7	10.0	10.0	10.0

and $R_{in2} = 1324.0$, $R_{in3} = 825.9$. In addition, the following resistors are needed with value and connections noted.

(*i*) 180.5 kΩ, node 2 of section 1 and node 1 of section 2.
(*ii*) 180.5 kΩ, node 1 of section 1 and node 4 of section 2.
(*iii*) 194.3 kΩ, node 2 of section 2 and node 1 of section 3.
(*iv*) 194.3 kΩ, node 1 of section 2 and node 4 of section 3.

---

* In practice, with the following modifications of Fig. 7, $R_{in3} = 825.9$ is used. Change the connection of sections 2 and 3 to between node 2 (section 2) and node 1′ (section 3); the connection of R_{f2} remains unchanged. Change the connection of R_{f3} to between node 2 (section 3) and the summing amplifier A_1.

REFERENCES

1. G. Hurtig, III, "The Primary Resonator Block Technique of Filter Synthesis," International Filter Symposium, Santa Monica, California, April 15–18, 1972, p. 84.
2. G. Hurtig, III, "Filter Network Having Negative Feedback Loops," United States Patent 3,720,881, March 13, 1973.
3. K. R. Laker and M. S. Ghausi, "Synthesis of a Low-Sensitivity Multiloop Feedback Active RC Filter," IEEE Trans. on Circuits and Systems, *CAS-21*, No. 2 (March 1974), pp. 252–259.
4. K. R. Laker, "On Multiparameter Sensitivity in Active RC Networks," Ph.D. Thesis, New York University, May 1973.
5. L. A. Zadeh and C. A. Desoer, *Linear System Theory: The State Space Approach*, New York: McGraw-Hill, 1963, pp. 282–283 and 357–358.
6. J. Tow and Y. L. Kuo, "Coupled Biquad Active Filters," IEEE Proc. International Symposium on Circuit Theory, N. Hollywood, California, April 18–21, 1972, pp. 164–168.
7. G. Szentirmai, "Synthesis of Multiple-Feedback Active Filters," B.S.T.J., *52*, No. 4 (April 1973), pp. 527–555.
8. J. J. Friend, "A Single Operational-Amplifier Biquadratic Filter Section," IEEE Proc. International Symposium on Circuit Theory, Digest of Technical Papers, December 1970, pp. 179–180.
9. C. L. Semmelman, E. D. Walsh, and G. T. Daryanani, "Statistical Circuit Design: Linear Circuits and Statistical Design," B.S.T.J., *50*, No. 4 (April 1971), pp. 1149–1171.
10. P. E. Fleischer and J. Tow, "Design Formulas for Biquad Active Filters Using Three Operational Amplifiers," Proc. Letters, IEEE, *61*, May 1973, pp. 662–663.
11. G. Szentirmai, private communication.